Reactive and Functional Polymers 161 (2021) 104846

Contents lists available at ScienceDirect

Reactive and Functional Polymers

journal homepage: www.elsevier.com/locate/react

Perspective Article

Biocompatible oligo-oxazoline crosslinkers: Towards advanced chitosans for controlled dug release

Mafalda Lopes [a], Rita Restani [a], Marco P. Carvalho [b,c], Ilídio Correia [b,c], Ana Aguiar-Ricardo [a], Vasco D.B. Bonifácio [d,*]

[a] LAQV-REQUIMTE, Departamento de Química, Faculdade de Ciências e Tecnologia, Universidade NOVA de Lisboa, Campus de Caparica, 2829-516 Caparica, Portugal
[b] CICS-UBI – Health Sciences Research Centre, Universidade da Beira Interior, Av. Infante D. Henrique, 6200-506, Covilhã, Portugal
[c] CIEPQF – Departamento de Engenharia Química, Universidade de Coimbra, Rua Sílvio Lima, 3030-790, Coimbra, Portugal
[d] iBB – Institute for Bioengineering and Biosciences, Instituto Superior Técnico, Universidade de Lisboa, 1049-001 Lisboa, Portugal

ARTICLE INFO

Keywords:
Oligo-oxazolines
Chitosan
Crosslinking
Supercritical carbon dioxide
Dexamethasone

ABSTRACT

Chitosan, a natural and abundant biopolymer has been long explored as a biocompatible material for the preparation of drug delivery devices. This strategy has been mostly accomplished using chemically crosslinked chitosan leading to more stable scaffolds. However, crosslinking has been shown to reduce both biocompatibility and swelling. In this work chitosan was crosslinked with novel biocompatible crosslinkers, based on oligo-oxazolines and glycidyl methacrylate copolymers, leading to patches with a very high swelling capacity. Dexamethasone therapeutics is strongly enhanced by a controlled release administration. This study shows that oligo-oxazoline-crosslinked chitosan is a suitable biomaterial for loading and controlled release of dexamethasone.

1. Introduction

Crosslinking is a powerful strategy to improve mechanical and chemical stability of engineered materials. Particular attention has been given to the production of biocompatible scaffolds using cross-linked natural polymers for the development of supports for tissue repair and regeneration, stem cell culture and drug delivery [1,2]. Chitosan (CHT) is a biocopolymer composed of randomly distributed *N*-acetylglucosamine and D-glucosamine units, varying in composition, sequence, and molecular weight. This outstanding polymer that has been the focus of many studies in the last decades, mainly due to its excellent biocompatibility, nontoxicity, biodegradability, mucoadhesion, antimicrobial properties, and importantly its easy modification [3]. Covalently crosslinked CHT hydrogels are a representative example of advanced biomaterials. However, the choice of safe crosslinkers (with well-documented biocompatibility and metabolism) is very limited, being a main disadvantage in the production of these systems. Also, crosslinking must overcome other issues such as low swelling or lack of controlled release under basic conditions (pH > 7). Common CHT crosslinkers include dialdehydes, like glutaraldehyde [4,5], as they stabilize CHT very efficiently [6]. Dialdehydes allow crosslinking in aqueous media, under moderate conditions, however a drastic decrease in bioadhesiveness [7] and an increase in toxicity [8] is mostly observed. Glutaraldehyde is toxic agent [9,10], and glutaraldehyde-crosslinked materials may present partially unreacted glutaraldehyde ends that were found to induce apoptosis [11], thus extensive purification in the crosslinking step is not enough to ensure safety of devices for human use. Despite some alternative crosslinkers, such as genipin [12–14], a natural but rather expensive agent, the development of novel low-cost, and fully biocompatible crosslinkers are still a challenge.

Many synthetic polymers used in hydrogel preparations such as poly (acrylic acid) (PAA), poly (hydroxyethyl methacrylate) (PHEMA), poly (vinyl alcohol) (PVA) and poly(ethylene glycol) (PEG), have a mucoadhesive and bioadhesive profile that increase the residence time of the drug and the tissue permeability. Adhesivity is due to chain interconnections that occur between the hydrogel and the mucus glycoproteins, thus enabling networks in specific locations, and drug administration can be carried out through oral, ocular, subcutaneous and transdermal routes. The transdermal delivery is a less aggressive and patient friendly choice with many advantages over the oral route: avoids pre-systemic liver metabolism, allows administration interruption by removing the system, enables the control of the release for a

* Corresponding author.
E-mail address: vasco.bonifacio@tecnico.ulisboa.pt (V.D.B. Bonifácio).

https://doi.org/10.1016/j.reactfunctpolym.2021.104846
Received 28 October 2020; Received in revised form 18 January 2021; Accepted 3 February 2021
Available online 7 February 2021
1381-5148/

longer period of time than the normal gastrointestinal transit of the oral dosage form, and the properties of the biological barrier to absorption may be tuned [15]. In this regard CHT an ideal material for transdermal applications since besides all the referred properties acts also as skin penetration enhancer by hydrating the stratum corneum [16].

Since the 1960s polyoxazolines have been the subject of research in wide range of applications, mostly in the biomedical field [17]. In the last decade the green synthesis of oligo-oxazolines (OOxs) using a supercritical carbon dioxide assisted polymerization [18], leading to oligomers with intrinsic blue fluorescence [19], opened new trends in the development of polyoxazoline-based materials [20].

Herein, we demonstrate for the first time the use of biocompatible oligo-oxazoline macromonomers (oligo-oxazolines having one end-group that enables its use as a monomer), as key intermediates in the crosslinking of CHT matrices.

2. Materials and methods

2.1. Materials

2-Ethyl-2-oxazoline (EtOx, ≥99%), boron trifluoride etherate ($BF_3{\cdot}OEt_2$), glycidyl methacrylate (GMA, 97%), 2,2′-azoisobutironitrile (AIBN, ≥ 98%), methacrylic acid (MAA, 99%), acetic acid, chitosan (CHT, 75–85% deacetylated, medium molecular weight), Phosphate-buffered saline pellets (PBS) and Lysozyme from chicken egg white (50.800 U/mg protein) were supplied by Sigma-Aldrich (Darmstadt, Germany). Triethylamine (Et_3N, ≥ 99%) and dexamethasone (≥ 97.0%) were purchased from Fluka (Darmstadt, Germany). Carbon dioxide (≥ 99.98%) was supplied by Air Liquide (Lisbon, Portugal). All the reagents were used as received.

2.2. Synthesis of oligo-oxazoline macromonomers

The oxazoline polymerizations followed our protocol [18]. Briefly, the oxazoline monomer (EtOx), the initiator ($BF_3.OEt_2$, 10% *v*/v) and a magnetic stirrer were placed in the high-pressure reactor which was subsequently immersed in a thermostated oil bath at 65 ± 0.01 °C, using a PID controller (Hart Scientific, Model 2000). The carbon dioxide was then inserted into the cell with a high-pressure compressor (NWA PM-101) to achieve the desired pressure, 18.5 MPa. After 24 h of reaction, the resulting polymer was washed continuously with CO_2 in order to eliminate catalyst and unreacted monomer residues. The pressure was slowly released, and the cell was cooled to room temperature. The *living* OOx was obtained as very hygroscopic yellow solid. As an example, for an initial volume of 2 mL of EtOx, 4 mL of acetonitrile, 860 μL of MAA and 2 mL of Et_3N were added. The solution was heated at 80 °C for 15 h. Acetonitrile was evaporated and the polymer redissolved in chloroform. This solution was washed with saturated aqueous sodium hydrogen carbonate solution and brine, dried over anhydrous sodium sulphate and filtered. After solvent removal under reduced pressure a brownish viscous polymer was obtained, which was stored at 4 °C to avoid decomposition.

The copolymerizations of OEtOx macromonomer and GMA, using three different percentages of GMA (25, 50 and 75 mol%), were carried out using a high-pressure cell under optimized conditions [21]. OEtOx macromonomer, 2 mol% EtOH (co-solvent with respect to CO_2) and a magnetic stirrer were inserted into the reactor and left to stir. After solubilization of the macromonomer, the GMA monomer and 5% AIBN initiator (w/w) were added. The cell was inserted in a thermostated oil bath at 65 °C and the desired pressure of 24 MPa was reached by CO_2 addition. After 24 h of reaction, the pressure was slowly released from the cell and cooled to room temperature. The copolymers obtained had a yellow colour and a viscous appearance.

The materials were characterized by FT-IR, NMR and GPC. The FT-IR spectra (Fig. S1) were recorded on a Perkin Elmer Spectrum 1000 spectrophotometer (Waltham, MA, USA), using potassium bromide (KBr) pellets, with a resolution of 1 cm^{-1} and 32 scans in the 4000 to 600 cm^{-1} range. The NMR spectra (Figs. S2, S3 and S4) were recorded on a Bruker ARX 400 MHz equipment (Karlsruhe, Germany). ^1H NMR chemical shifts are reported as δ (ppm = parts per million) relative to the residual solvent peak. The number average molecular weight (M_n) and the polydispersity index (PDI) was determined for the **OOX_{70}** copolymer by GPC on a Knauer system equipped with a Smartline Autosampler 3800 (Berlin, Germany), a HPLC Smartline Pump 1000 (Berlin, Germany) and a PL-ELS detector from Polymer Laboratoires (San Diego, CA, USA) using dimethylformamide as solvent at a flow rate of 1 $mLmin^{-1}$ on a PlusPore column (7.5 mm id) from Agilent (Santa Clara, CA, USA) at 85 °C. The system was calibrated with polystyrene standards. The obtained values, M_n = 16,211 $gmol^{-1}$ (n = 12) and PDI = 1.2, were in accordance with our previous data reported for $scCO_2$-assisted oxazoline polymerizations.

2.3. Chitosan crosslinking

The matrices were crosslinked in a cylindrical glass mold (dxh = 1.2 × 3.0 cm), with different compositions of CHT and crosslinker (10, 30 and 50% *w*/w relative to CHT) using a total mass of approximately 90 mg (*e.g.* 80 mg of CHT and 8 mg of OOx_{70} crosslinker for the preparation of **CHT-10OOx_{70}**) and 3 mL of aqueous acetic acid solution 1% (*v*/v). The mixtures were left under magnetic stirring at 60 °C for 24 h. After this period the mixtures were frozen for 20 min at −20 °C and then lyophilized until dry using a TELSTAR CRYODOS -50, as reported [22].

2.4. Stability assays

Samples of crosslinked scaffolds (approximately 30 mg) were immersed in 50 mL of a PBS solution (pH = 7.4) containing 2 μg/mL of lysozyme at 37 °C. The samples were periodically removed from the solution, frozen (20 min. at −20 °C), lyophilized and weighed. The procedure was repeated for a period of 30 days (or shorter in the cases of faster degradation), renewing the PBS-lysozyme solutions after this procedure. Following the same methodology, the pH stability of the scaffolds was evaluated in PBS solution (pH = 7.4) and in sodium acetate 0.2 M solution (pH = 5.0). For both assays the remaining mass of each sample was calculated using Eq. (1):

$$M(\%) = \frac{M_r}{M_0} \times 100 \quad (1)$$

where M_r is the recovered mass and M_0 is the initial mass. The scaffolds swelling capacity was also evaluated under two swelling cycles (12 and 24 h). Samples of crosslinked scaffolds (approximately 30 mg) were immersed in 50 mL of a PBS solution (pH = 7.4) at 37 °C according to literature [23]. In the 24 h swelling cycle the weighings were carried out every 20 min in the first hour, carefully removing excess solution before weighing (drainage in absorbent paper). After the first hour, the weighings were carried out hourly, until 24 h. After this period, the temperature of the immersion bath was changed to 20 °C and procedure repeated. Then, the temperature was changed again to 37 °C and the procedure repeated up to 78 h. In the 12 h swelling cycle, weighings were carried out every 30 min for 6 h using the procedure described above. This procedure was repeated until 21 h. The scaffolds swelling was calculated using Eq. (2):

$$\text{Swelling}\ (\%) = \frac{M_i - M_d}{M_d} \times 100 \quad (2)$$

where M_i is the mass after immersion and M_d is the dried mass.

2.5. Scaffolds characterization

The morphology of the scaffolds was recorded using scanning electron microscopy (SEM) in a Hitachi S-2400 instrument (Tokyo, Japan), with an accelerating voltage set to 15 kV. The scaffold samples were

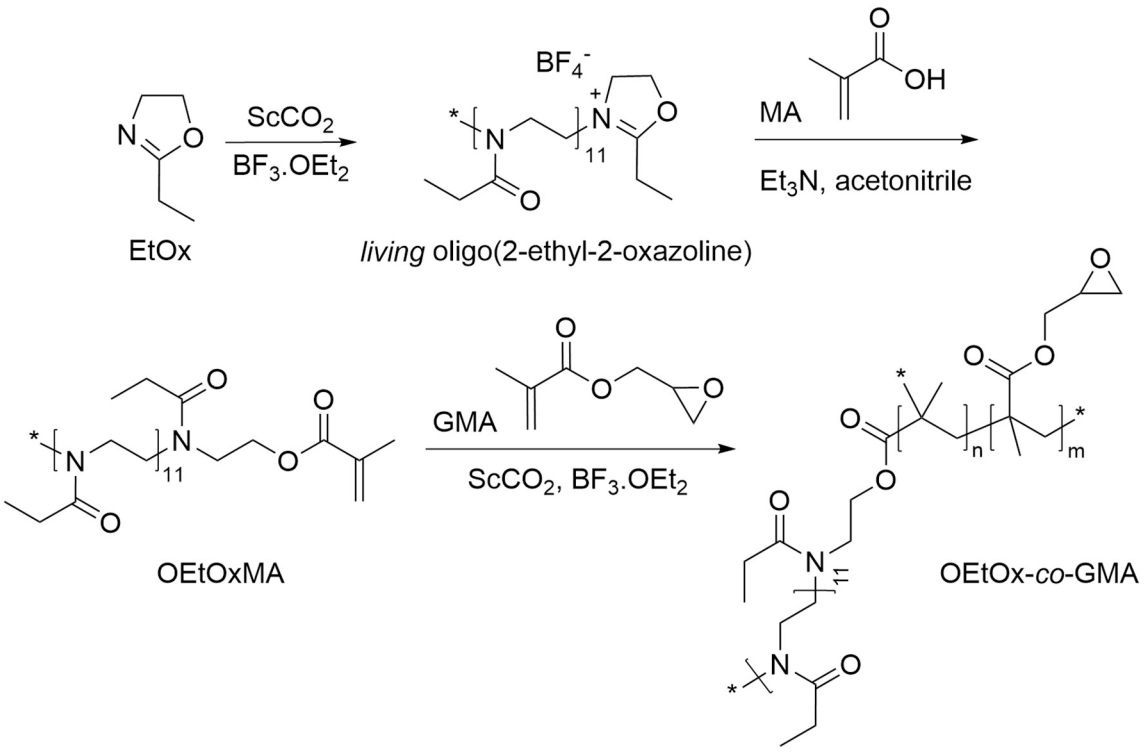

Scheme 1. Synthesis of oligo-oxazoline crosslinkers.

frozen and fractured in liquid nitrogen for cross-section analysis. All samples were coated with gold before analysis.

2.6. Biocompatibility assays

Scaffolds biocompatibility was assessed through the MTS assay following ISO 10993–5 (Biological evaluation of medical devices-Part 5: Tests for *in vitro* cytotoxicity). Briefly, scaffolds ($n = 5$) were placed in 96-well plates, occupying <10% of the well area, and then were sterilized under UV irradiation (254 nm, ~7mWcm^{-2}) over 1 h. Subsequently, NHDF cells (PromoCell®) were seeded at a density of 10×10^3 cells/well in the presence of the scaffolds and 100 μL fresh culture medium were added to each well. Hereafter, cell culture plates were incubated at 37 °C, in a 5% CO_2 humidified atmosphere. After 24 and 48 h of cells being seeded in contact with scaffolds, the medium of each well was removed and replaced with a mixture of 100 μL of fresh culture medium and 20 μL of MTS/PMS (phenazine methosulfate) reagent solution. After 4 h of incubation at 37 °C, in a 5% CO_2 atmosphere, the absorbance of each sample was determined at 492 nm using a microplate reader (Biorad xMark™ microplate spectrophotometer). Cells incubated without materials were used as a negative control (K^-), whereas cells incubated with EtOH (96%) were used as positive control (K^+). Optical and scanning electron microscopic analysis was also performed to characterize cell adhesion and proliferation at the surface of the produced scaffolds.

2.7. Dexamethasone loading and controlled release

The scaffolds were crosslinked in a cylindrical glass mold ($d \times h = 1.2 \times 3.0$ cm), using different CHT and crosslinker ratios (*w*/w) with a total mass of approximately 90 mg and 3 mL of an aqueous solution of acetic acid 1% (*v*/v). The mixtures were left under magnetic stirring at 60 °C for 24 h. Next, 6 mg of dexamethasone were added to each solution and left to stir for more 24 h at room temperature. After this period the mixtures were frozen for 20 min at −20 °C and lyophilized. Samples of approximately 30 mg of the crosslinked scaffolds loaded with dexamethasone were immersed in 50 mL of phosphate-saline buffer solution (PBS, pH = 7.4) at 35 °C. Samples of 1 mL were taken every 30 min for 2 h and then hourly until 27 h. After each sample withdrawn, 1 mL of fresh PBS solution was added (1:50 dilution ratio, negligible for concentration calculations). The release of dexamethasone over time was followed by absorbance measurements at 242 nm. A calibration curve was constructed using the same experimental conditions.

3. Results and discussion

3.1. Synthesis of oligo-oxazoline macromonomers

The oxazoline polymerizations followed a $scCO_2$-assisted cationic ring-opening polymerization (CROP) protocol [18]. Under these conditions the CROP of oxazolines leads to the formation of *living* oligomers allowing a final termination of highly reactive ends with a desired nucleophilic species. Thus, using triethylamine (Et_3N) as a base, we prepared the methacrylamide acid ammonium salt and obtained the corresponding oligo-oxazoline macromonomer using our optimized protocol [21]. Next, oligo(2-ethyl-oxazoline) macromonomer (OEtOxMA) and glycidyl methacrylate (GMA) were copolymerized varying the OEtOxMA:GMA feed ratio (75:25, 50:50 and 25:75) (Scheme 1).

The materials were characterized by FT-IR, ^{1}H NMR and GPC. The FT-IR spectra of oligo(2-ethyl-2-oxazoline) methacrylate (OEtOxMA) show the characteristic amide band at *ca.* 1590 cm^{-1}. The presence of OH groups at *ca.* 3478 cm^{-1} was also observed after epoxide hydrolysis of the copolymers under crosslinking optimization studies (Fig. S1).

The OEtOx polymerization degree ($n = 12$) was determined by the integration of the signals corresponding to the double bond protons (acrylate terminal end, Ha/Ha') relatively to the methylene protons of the oligo-oxazoline (main chain, Hc) (Fig. S2a). The success of the copolymerization was confirmed by the presence of the GMA epoxide ring protons at 3.22 (Ha), 2.84 (Hb) and 2.63 (Hb') ppm (Fig. S2b). The copolymers composition was calculated by integration of these protons relatively to the methylene protons of the oligo-oxazoline at 3.5 ppm.

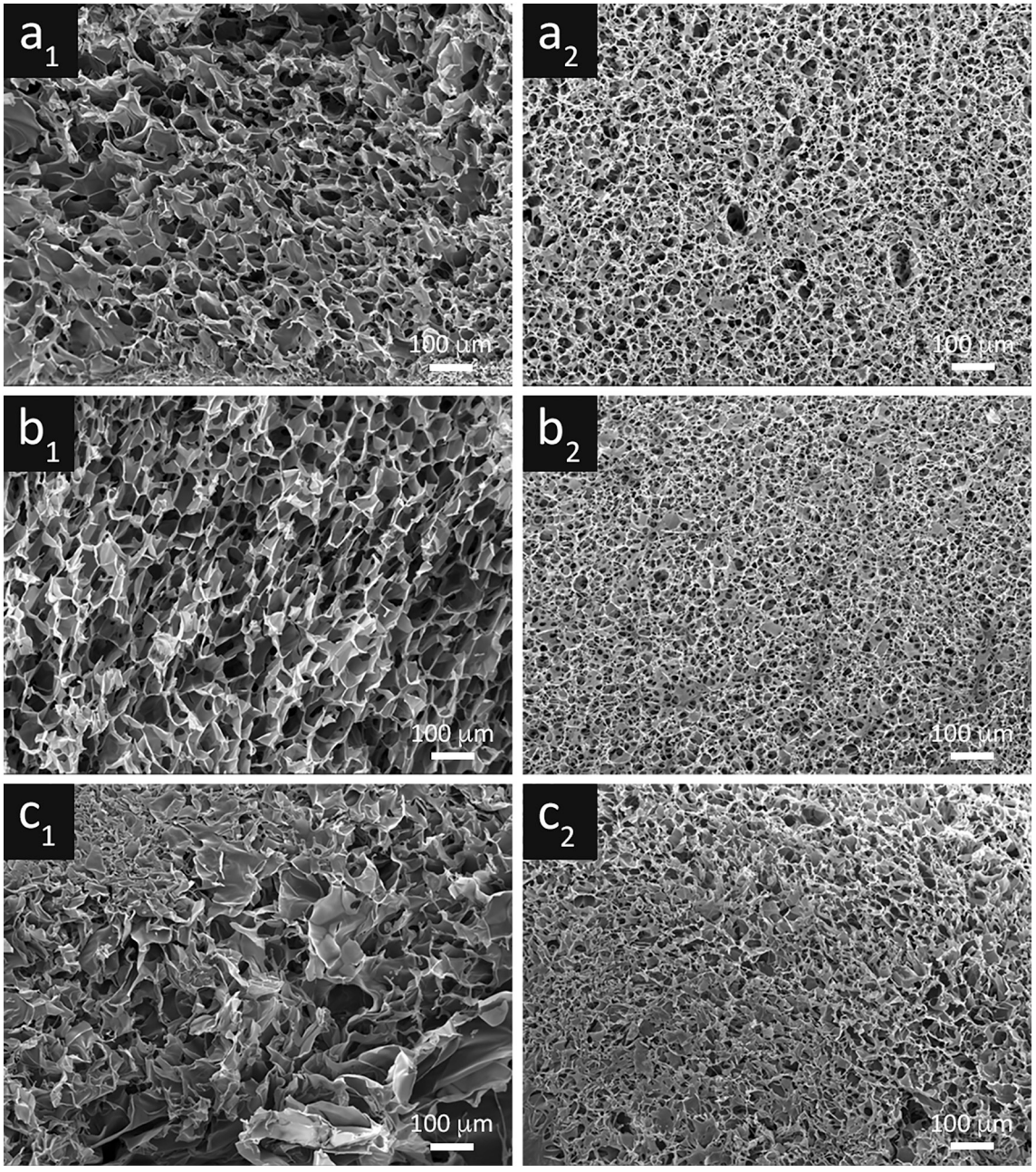

Fig. 1. SEM images showing the cutting section (1) and surface (2) of chitosan OOx-crosslinked scaffolds: **CHT-10OOx$_{70}$** (a), **CHT-30OOx$_{70}$** (b) and **CHT-50OOx$_{70}$** (c) (100× magnification).

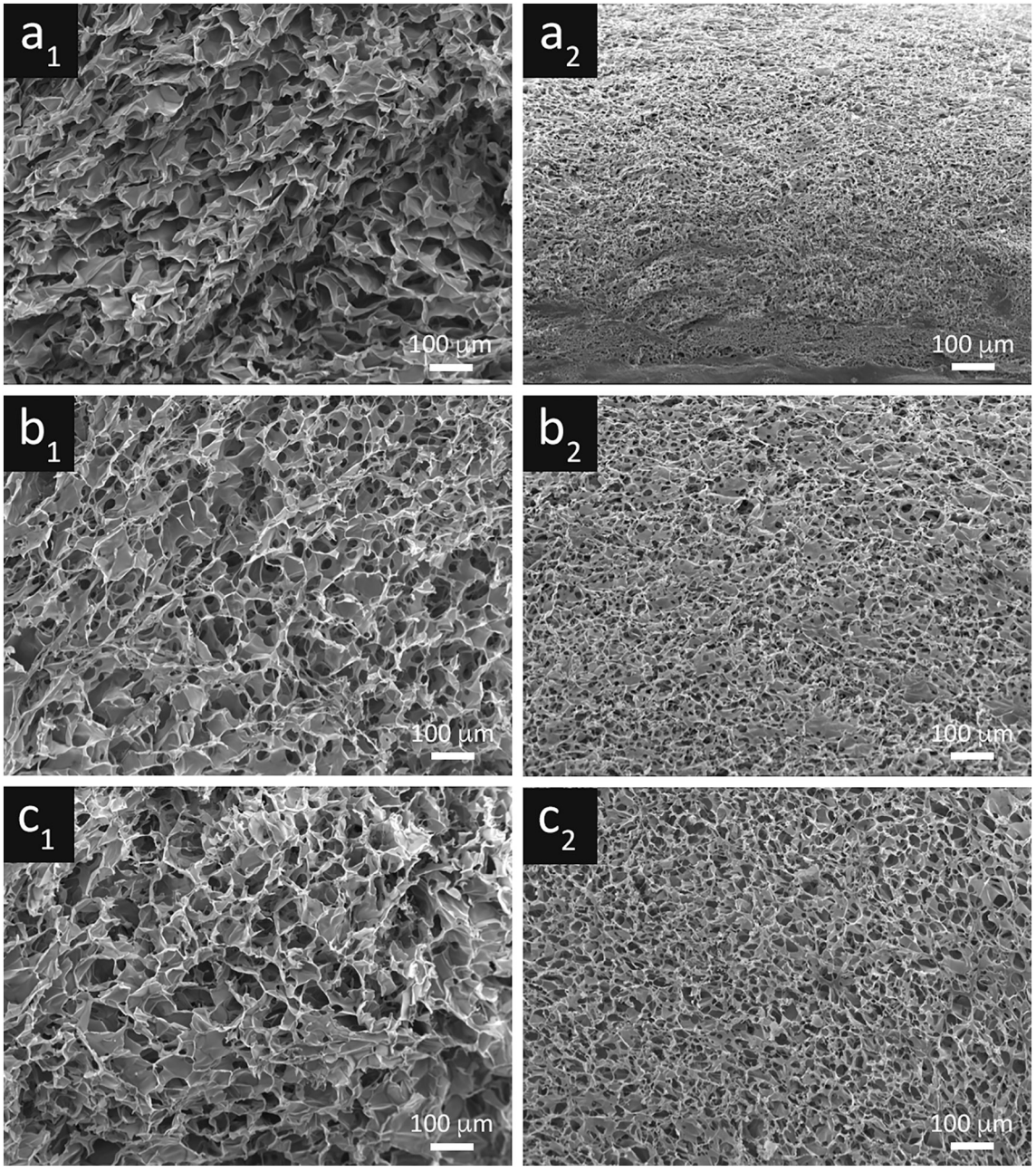

Fig. 2. SEM images showing the cutting section (1) and surface (2) of chitosan OOx-crosslinked scaffolds: **CHT-10OOx$_{45}$** (a), **CHT-30OOx$_{45}$** (b) and **CHT-50OOx$_{45}$** (c) (100× magnification).

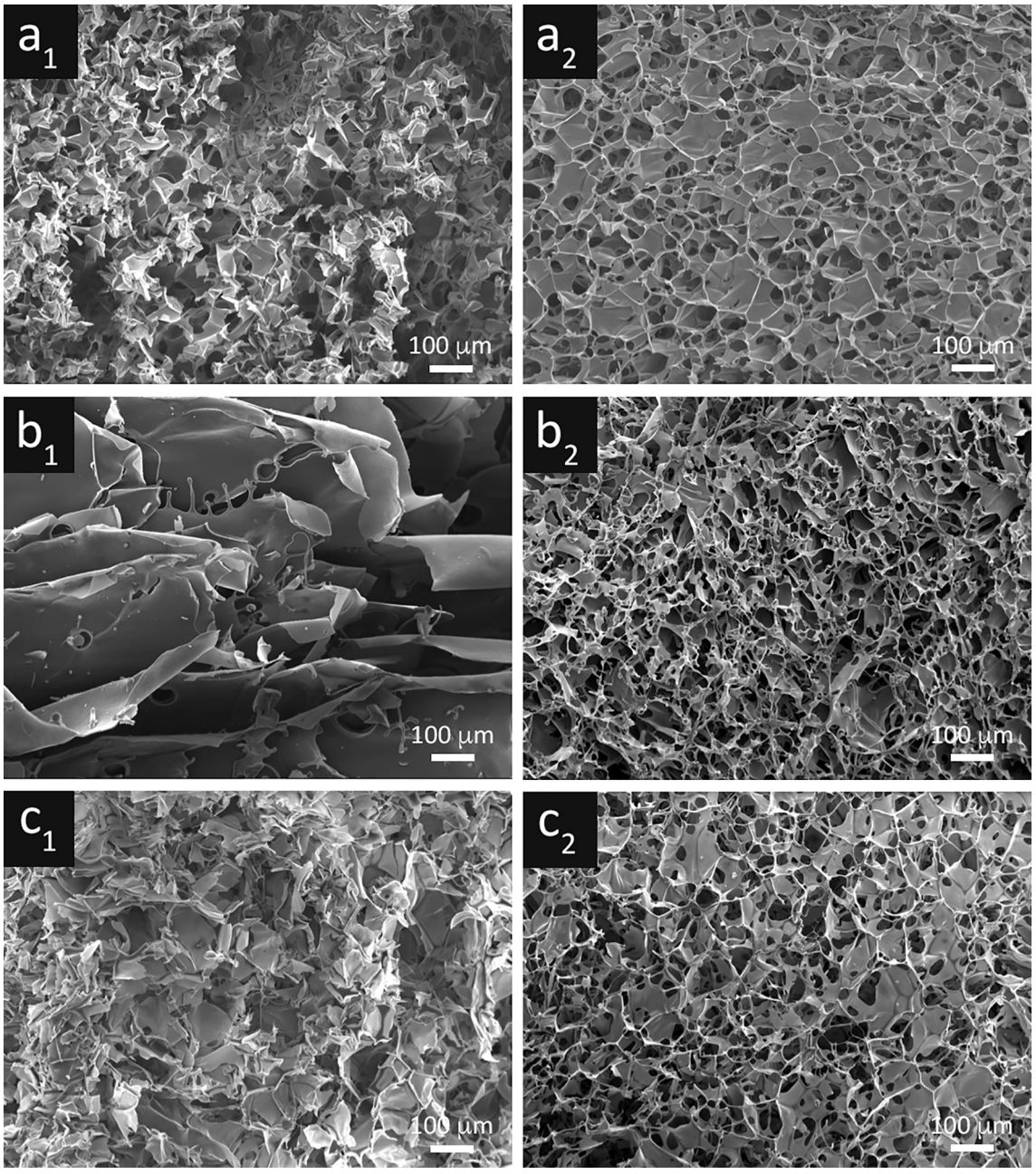

Fig. 3. SEM images showing the cutting section (1) and surface (2) of chitosan OOx-crosslinked scaffolds: **CHT-10OOx$_{25}$** (a), **CHT-30OOx$_{25}$** (b) and **CHT-50OOx$_{25}$** (c) (100× magnification).

The obtained OEtOx:GMA ratios were calculated by ^{1}H NMR by the integration of the GMA epoxide proton relative to the OEtOx methylene protons. The copolymers composition, determined by NMR, was found to be very similar to the monomers feed ratio: OEtOx-*co*-GMA 70:30 (**OOx$_{70}$**) from 75:25, OEtOx-*co*-GMA 45:55 (**OOx$_{45}$**) from 50:50 and OEtOx-*co*-GMA 25:75 (**OOx$_{25}$**) from 25:75.

Before chitosan crosslinking, we studied the crosslinking conditions using GMA as a model monomer. This study was carried out under the experimental conditions commonly used in the crosslinking reaction involving chitosan matrices, and we selected an aqueous solution of 1% acetic acid (*v*/v), 24 h and 60 °C as the optimal conditions. Under acidic conditions the epoxide oxygen in the GMA is protonated, and ring opening occurs by the nucleophilic attack of a water molecule. As expected, under these conditions the epoxide ring was found to originate the corresponding diol in quantitative yield. The success of the reaction was assessed by ^{1}H NMR. The peaks corresponding to the protons from the epoxide ring disappeared and new peaks characteristic of methylene protons adjacent to a diol appeared (Fig. S3a). The copolymer **OOx$_{25}$** was also easily hydrolysed under the same experimental conditions (Fig. S3b-c).

3.2. Chitosan biocompatible crosslinking

Due to its high reactivity, epoxides are prone to easy nucleophilic addition, especially in the presence of highly nucleophilic primary amines. This strategy was previously explored in the copolymerization of chitosan with GMA, which was found to be a suitable support for urease immobilization [24]. In this work, we synthesised oligo-oxazolines copolymerized with GMA and studied its effect on chitosan crosslinking. The chosen percentages of crosslinker (**OOx$_{70}$**,**OOx$_{45}$** and

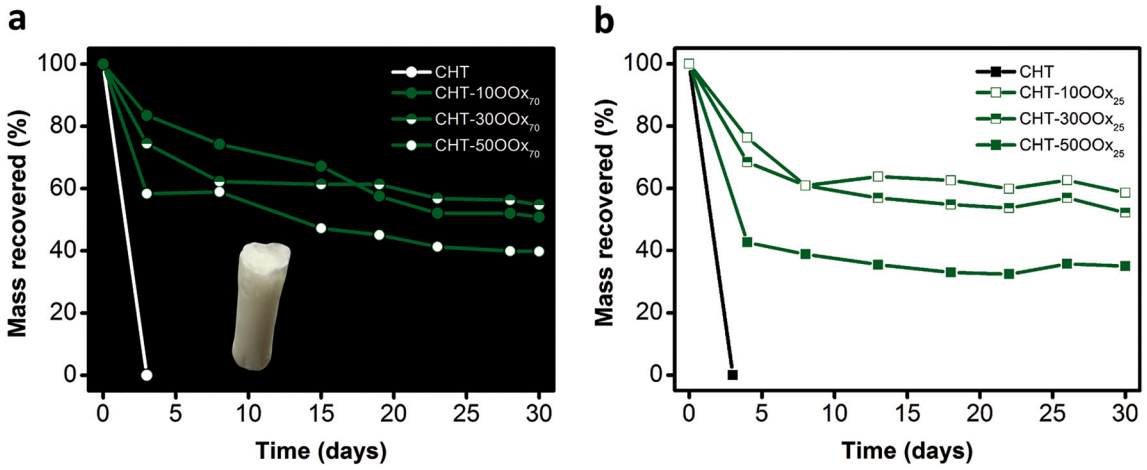

Fig. 4. Enzymatic degradation of chitosan OOx-crosslinked scaffolds using lysozyme at 37 °C for 30 days: **CHT-10OOx$_{70}$,CHT-30OOx$_{70}$,CHT-50OOx$_{70}$** (a) and **CHT-10OOx$_{25}$,CHT-30OOx$_{25}$,CHT-50OOx$_{25}$** (b). The inset picture shows a scaffold before the assay.

OOx$_{25}$) relatively to chitosan were 10, 30 and 50% (*w*/w), leading to 9 matrices: **CHT-10OOx$_{70}$,CHT-30OOx$_{70}$,CHT-50OOx$_{70}$,CHT-10OOx$_{45}$, CHT-30OOx$_{45}$,CHT-50OOx$_{45}$,CHT-10OOx$_{25}$,CHT-30OOx$_{25}$** and **CHT-50OOx$_{25}$.**

The crosslinking was confirmed by ^{1}H NMR using the **CHT-50OOx$_{25}$** scaffold. The spectra of CHT and **CHT-50OOx$_{25}$** were recorded using a 20% CD_3CO_2D (*v*/v) solution in D_2O, at room temperature. The CHT degree of acetylation was found to be 80%. This value was calculated by integration of the protons of the *N*-acetyl group, singlet at 1.91 ppm (2.07 ppm at 70 °C [25]) and the H-2 proton, singlet at 3.01 ppm (Fig. S4a). After reticulation the scaffolds become highly insoluble, therefore we performed the degradation of **CHT-50OOx$_{25}$** with lysozyme for a period of 30 days. Then, after washing with water and lyophilization it was possible to acquire the ^{1}H NMR spectrum of a partially crosslinked CHT, which showed the characteristic signals from CHT and the copolymer (Fig. S4b). A higher resolution spectrum also indicates the presence of materials with lower molecular weight, as a result of biodegradation. This characterization allowed us to confirm a successful covalent crosslinking (discarding blending), otherwise after CHT breaking down the copolymer would be released into the media and removed in the wash out since acidic hydrolysis turns the copolymers highly soluble in water.

After lyophilization, white scaffolds with a rough surface and a spongy porous structure were obtained. The morphology was analysed by SEM (Figs. 1-3). As expected porosity increases with increasing crosslinker concentration (*e.g.* 22.5 mm, 27.5 mm and 45 mm porous average diameter for **CHT-10OOx$_{70}$, CHT-30OOx$_{70}$** and **CHT-50OOx$_{70}$,** respectively; values calculated with *Image J* using SEM cross-section images) in agreement with previous studies [26], which may be explained by the decrease in the fraction of the real volume occupied by the material itself when CHT concentration decreases. This demonstrates that the CHT microstructure can be adjusted by varying its concentration through scaffold preparation. For the same crosslinker concentration it can be seen that there is no significant change in porosity, either in the cutting section or on the surface, when the GMA content is increased from 30 to 55% (**CHT-OOx$_{70}$** and **CHT-OOx$_{45}$**,*cf.* Figs. 2b$_1$-b$_2$, 2c$_1$-c$_2$, 3b$_1$-b$_2$, 3c$_1$-c$_2$). In scaffolds crosslinked with OOx copolymers having higher GMA concentration (**CHT-OOx$_{25}$**, Fig. 3) a significant increase in porosity is observed.

To further evaluate the potential of OOx-crosslinked CHT scaffolds as biocompatible drug delivery patches, biodegradation, stability and swelling tests were carried out at 37 °C at pH 7.4 for 30 days under different conditions. Enzymatic assays using lysozyme shown that scaffolds suffered a degradation between 35 and 60%, being the degradation more pronounced for scaffolds with higher crosslinking content (Fig. 4).

The higher degradation may be attributed to a much porous structure resulting in higher absorption by the lysozyme solution and therefore a larger exposition to the enzyme [27]. The pH stability at pH = 5 and pH = 7.4 (Fig. S5) was evaluated periodically for a 30 days period using the scaffolds which showed lower biodegradation, being selected the scaffolds prepared with 10% of crosslinker (**CHT-10OOx$_{25}$,CHT-10OOx$_{45}$** and **CHT-10OOx$_{70}$**). Non-crosslinked CHT, used as a control, become soluble in the medium after 3 days. The same result was observed for pH 5, where all the scaffolds lost its structure and become soluble in the medium after 3 days. For pH 7.4 a different behaviour was observed (Fig. S5). The scaffold with higher content of GMA (**CHT-10OOx$_{25}$**), which allow a higher crosslinking degree was found to be the most stable (~50% recovered mass after 30 days of periodic manipulation). In a control experiment were scaffolds were only analysed after 30 days, without periodic manipulation, the recovered mass was 80–85%.

In general, the scaffolds showed a very high swelling capacity (*e.g.* 1644% for **CHT-50OOx$_{70}$**, pH = 7.4), if compared with CHT glutaraldehyde-crosslinked scaffolds (*e.g.* 75% using 8 mol% glutaraldehyde, pH = 7), which is *ca.* 20-fold increase, or with non-crosslinked CHT scaffolds (650%, pH = 7) [28]. To the best of our knowledge this is the first report of a CHT crosslinking-triggered swelling enhancement. This extraordinary swelling rate is attributed to the hydrophilic nature of OOxs.

Cell adhesion assays revealed that OOx crosslinking did not affected the scaffolds biocompatibility. Fig. 5 shows SEM pictures taken after 1 and 3 days of incubation of Normal Human Dermal Fibroblasts (NHDF) cells with selected scaffolds. Cell adhesion was found to increase both with the increasing content of GMA in the crosslinker (70% *versus* 55%, **OO$_{x25}$** and **OO$_{x45}$**, respectively) and the increasing content of crosslinker (30% *versus* 50% *w*/w, **CHT-30OO$_{x25}$** and **CHT-50OO$_{x25}$**, respectively). This means that highly crosslinked scaffolds having a lower CHT content, as in the case of **CHT-30OOx$_{25}$** (Fig. 5c), display a stronger cell adhesion. In these scaffolds we can also distinguish three different behaviours: i) scaffold **CHT-50OOx$_{45}$** enables a week adhesion, cells only touch CHT surfaces, ii) scaffold **CHT-50OOx$_{25}$** enables a good adhesion, cells are flattened and more elongated, and iii) scaffold **CHT-30OOx$_{25}$** enables both adhesion and proliferation.

MTS assays and incubation with human fibroblasts also confirmed the scaffolds biocompatibility (Figs. S6 and S7).

3.3. Dexamethasone loading and controlled delivery

Dexamethasone is a synthetic glucocorticoid that has been used routinely as a key component in osteogenic differentiation protocols and

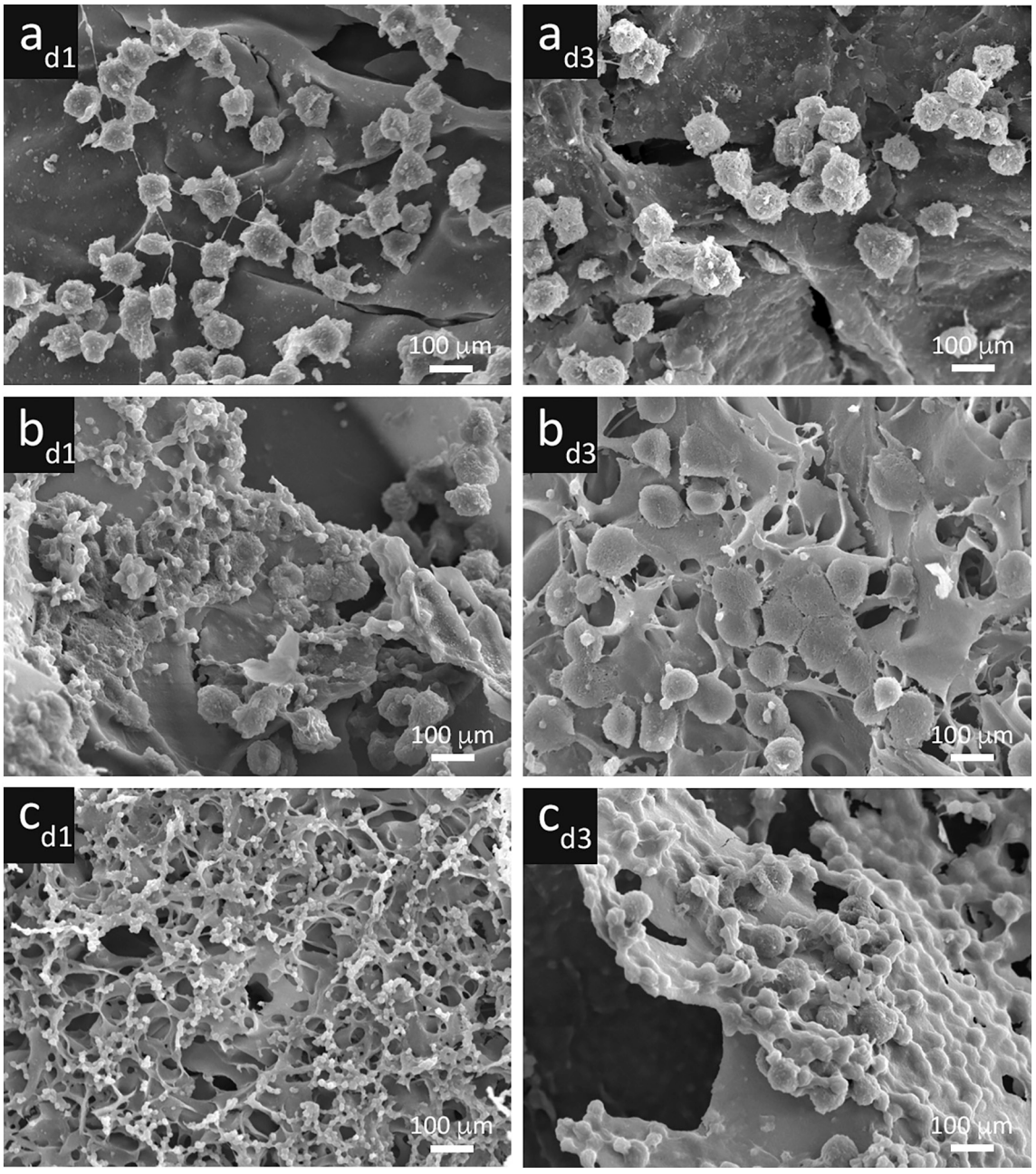

Fig. 5. SEM images of NHDF cells cultured in chitosan OOx-crosslinked scaffolds at day 1 (d1) and day 3 (d3): **CHT-50OOx$_{45}$** (a), **CHT-50OOx$_{25}$** (b) and **CHT-30OOx$_{25}$** (c).

in the treatment of many pathologies. Very recently, it was also demonstrated to be very efficient in the treatment of COVID-19 [29]. Oral administration poses several limitations, such as small daily doses (0.5–9 mg), hepatic first pass effect, enzymatic inactivation and gastric irritation [30]. Commercial dexamethasone formulations for topical use include gels, a more suitable administration to avoid complications from a systemic treatment [31]. However, they are not suitable for prolonged, controlled release through intact skin [32], and the controlled release from different materials has been fairly investigated.

In our study dexamethasone was impregnated in OOx-crosslinked chitosan scaffolds prepared by freeze-drying, taking in account the maximum recommended daily dose (6 mg). The release assays were carried out in a PBS solution at 35 °C for 27 h. The release profile and the calibration curve (Fig. S8) were obtained following the absorption maximum of dexamethasone (λ_{max} = 242 nm) in PBS solution. All samples used in the release studies were sectioned from the lower part of the scaffold, which may be assumed to have a higher dexamethasone concentration if compared with the upper section. Fig. 6 shows the dexamethasone release profile of CHT OOx-crosslinked scaffolds.

Interestingly, a more sustained release (*ca.* 60% release after 24 h) was observed for the scaffolds having the highest CHT content (90%) and the higher crosslinking degrees (**CHT-10OOx$_{70}$** and **CHT-10OOx$_{45}$**, solid circles in Fig. 6), which correspond to less porous structures. As expected, a less sustained release was observed for the scaffolds with the highest GMA content, independently of the CHT concentration (**CHT-10OOx$_{25}$**,**CHT-30OOx$_{25}$** and **CHT-50OOx$_{25}$**). Higher porosity leads to higher water diffusion into the polymeric matrix, thus facilitating drug diffusion (*ca.* ~90% release after 8 to 10 h). The first 60% dexamethasone release curve acted as a perfect sink under pseudo steady-state conditions and was analysed using the Higuchi simplified equation

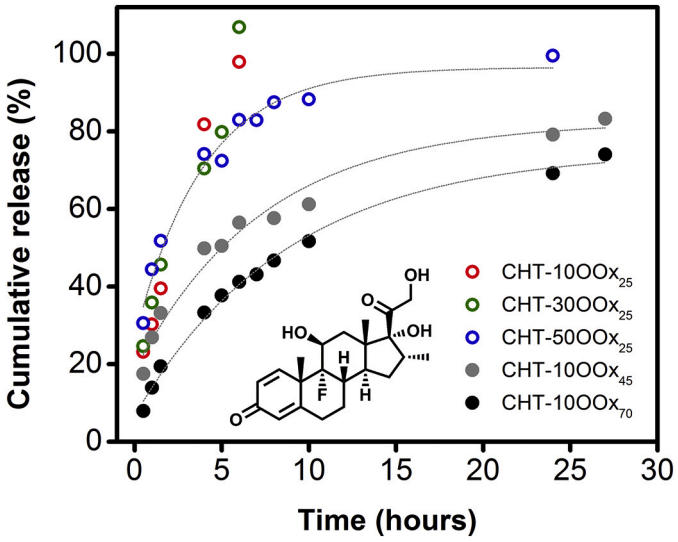

Fig. 6. Dexamethasone cumulative release from chitosan OOx-crosslinked scaffolds. Release profile from scaffolds with the same amount of crosslinker but different crosslinking rate and from scaffolds with different amount of crosslinker but the same crosslinking rate. The inset shows the chemical structure of dexamethasone.

($M_t = K\ t^{1/2}$) [33]. Dexamethasone release fitted the Higuchi model, suggesting that the release is controlled by a pore-mediated diffusion process, thus indicating that the release rate is dependent on the matrix porosity (Fig. S9).

4. Conclusions

Novel biocompatible crosslinkers were synthesised by copolymerization of different ratios of an oligo-oxazoline macromonomer and glycidyl methacrylate. These crosslinkers were investigated as new chitosan crosslinking agents and showed excellent biocompatibility and swelling capacity. Crosslinking tuning, varying the chitosan:crosslinker ratio and the crosslinker ability, enable the production of patches with stability for 30 days at pH 7.4, cell adhesion and proliferation, and dexamethasone-controlled delivery for more than 24 h. Overall, these advanced chitosan-based materials show a great potential for transdermal drug delivery.

Declaration of Competing Interest

The authors declare that they have no known competing financial interests or personal relationships that could have appeared to influence the work reported in this paper.

Acknowledgements

This research was funded by Fundação para a Ciência e a Tecnologia (FC&T, Portugal) through projects PTDC/QUI/73939/2006 and PTDC/CTM/099452/2008, and also funded by Associate Laboratory for Green Chemistry - LAQV which is financed by national funds from FCT/MCTES (UIDB/50006/2020 and UIDP/50006/2020). We also thank André F. Moreira for the porosity analysis of the chitosan patches using *Image J*.

Appendix A. Supplementary data

Supplementary data to this article can be found online at https://doi.org/10.1016/j.reactfunctpolym.2021.104846.

References

[1] Y. Zhu, T. Liu, K. Song, B. Jiang, X. Ma, Z. Cui, Collagen-chitosan polymer as a scaffold for the proliferation of human adipose tissue-derived stem cells, J. Mater. Sc. Mater. Med. 20 (2009) 799–808, https://doi.org/10.1007/s10856-008-3636-6.
[2] M. Temtem, L.M.C. Silva, P.Z. Andrade, F. Santos, C. Lobato da Silva, J.M.S. Cabral, M.M. Abecasis, A. Aguiar-Ricardo, Supercritical CO_2 Generating Chitosan Devices with Controlled Morphology, Potential Application for Drug Delivery and Mesenchymal Stem Cell Culture, J. Supercrit. Fluids 48 (3) (2009) 269–277, https://doi.org/10.1016/j.supflu.2008.10.020.
[3] M.M. Raja, P.Q. Lim, Y.S. Wong, G.M. Xiong, Y. Zhang, S. Venkatraman, Y. Huang, Polymeric nanomaterials: methods of preparation and characterization, Nanocarriers for drug delivery (2019) 557–653, https://doi.org/10.1016/B978-0-12-814033-8.00018-7.
[4] V.R. Patel, M.M. Amiji, Preparation and characterization of freeze-dried chitosan-poly(ethylene oxide) hydrogels for site-specific antibiotic delivery in the stomach, Pharm. Res. 13 (1996) 588–593, https://doi.org/10.1023/A:1016054306763.
[5] A.S. Aly, Self-dissolving chitosan, I. Preparation, characterization and evaluation for drug delivery system, Angew. Makromol. Chem 259 (1) (1998) 13–18, https://doi.org/10.1002/(SICI)1522-9505(19981001)259:1<13::AID-APMC13>3.0.CO;2-T.
[6] J. Berger, M. Reist, J.M. Mayer, O. Felt, N.A. Peppas, R. Gurny, Structure and interactions in covalently and ionically crosslinked chitosan hydrogels for biomedical applications, Eur. J. Pharm. Biopharm. 57 (1) (2004) 19–34, https://doi.org/10.1016/s0939-6411(03)00161-9.
[7] I. Genta, M. Constantitni, A. Asti, B. Conti, L. Montanari, Influence of glutaraldehyde on drug release and mucoadhesive properties of chitosan microspheres, Carbohydr. Polym. 36 (2–3) (2000) 81–88, https://doi.org/10.1016/S0144-8617(98)00022-8.
[8] B. Carreño-Gómez, R. Duncan, Evaluation of biological properties of soluble chitosan and chitosan microspheres, Int. J. Pharm 148 (82) (1997) 231–240, https://doi.org/10.1016/S0378-5173(96)04847-8.
[9] B. Ballantyne, S.L. Jordan, Toxicological, medical and industrial hygiene aspects of glutaraldehyde with particular reference to its biocidal use in cold sterilization procedures, J. Appl. Toxicol. 21 (2) (2001) 131–151, https://doi.org/10.1002/jat.741.
[10] R.O. Beauchamp, M.B. St Clair, T.R. Fennel, D.O. Clarke, K.T. Morgan, A critical review of the toxicology of glutaraldehyde, Crit. Rev. Toxicol. 22 (3–4) (1992) 143–174, https://doi.org/10.3109/10408449209145322.
[11] J.E. Gough, C.A. Scotchford, S. Downes, Cytotoxicity of glutaraldehyde crosslinked collagen/poly(vinyl alcohol) films is by the mechanism of apoptosis, J. Biomed. Mater. Res. 61 (1) (2002) 121–130, https://doi.org/10.1002/jbm.10145.
[12] F. Mi, Y. Tan, H. Liang, R. Huang, H. Sung, In vitro evaluation of a chitosan membrane cross-linked with genipin, J. Biomater. Sci. Polym. Ed. 12 (8) (2001) 835–850, https://doi.org/10.1163/156856201753113051.
[13] J. Kawadkar, M.K. Chauhan, Intra-articular delivery of genipin cross-linked chitosan microspheres of flurbiprofen: preparation, characterization, in vitro and in vivo studies, Eur. J. Pharm. Biopharm. 81 (3) (2012) 563–572, https://doi.org/10.1016/j.ejpb.2012.04.018.
[14] Y. Zhang, Y. Yu, X. Shi, S. Zhao, A. Chen, D. Huang, D. Niu, Z, Qin, study on the preparation of genipin crosslinked chitosan microspheres of resveratrol and in vitro release, J. Polym. Res. 20 (2013) 175, https://doi.org/10.1007/s10965-013-0175-8.
[15] N. Kanikkannan, K. Kandimalla, S.S. Lamba, M. Singh, Structures activity relationship of chemical penetration enhancers in transdermal drug delivery, Curr. Med. Chem. 7 (6) (1999) 593–608, https://doi.org/10.2174/0929867003374840.
[16] A. Praveen, M. Aqil, in: S. Jana, S. Jana (Eds.), Transdermal delivery of chitosan-based systems in functional chitosan, Springer, Singapore, 2019.
[17] M. Glassner, M. Vergaelen, R. Hoogenboom, Poly(2-oxazoline)s: a comprehensive overview of polymer structures and their physical properties, Polym. Int. 67 (1) (2018) 32–45, https://doi.org/10.1002/pi.5457.
[18] C. Veiga de Macedo, M.S. Silva, T. Casimiro, E.J. Cabrita, A. Aguiar-Ricardo, Boron trifluoride catalyzed polymerization of 2-substituted-2-oxazolines in supercritical carbon dioxide, Green Chem. 9 (2007) 948–953, https://doi.org/10.1039/B617940A.
[19] V.D.B. Bonifácio, V.G. Correia, M.G. Pinho, J.C. Lima, A. Aguiar-Ricardo, Blue emission of carbamic acid oligooxazoline biotags, Mater. Lett. 81 (2012) 205–208, https://doi.org/10.1016/j.matlet.2012.04.134.
[20] A. Aguiar-Ricardo, V.D.B. Bonifácio, T. Casimiro, V.G. Correia, Supercritical carbon dioxide design strategies: from drug carriers to soft killers, Philos. Trans. A Math. Phys. Eng. Sci. 373 (2015) 20150009, https://doi.org/10.1098/rsta.2015.0009.
[21] R. Restani, Development of 2-Oxazoline-Based Hydrogels and Porous Polyester Microparticles in Supercritical CO_2, Faculdade de Ciências e Tecnologia – Universidade Nova de Lisboa, Master Thesis, 2009.
[22] M.C. Lígia, Silva, Development of Chitosan and Poly(Vinyl Alcohol) Blended Scaffolds for Cell Culture Using Supercritical Fluids Technology, Faculdade de Ciências e Tecnologia – Universidade Nova de Lisboa, Master Thesis, 2008.
[23] M. Temtem, T. Casimiro, J.F. Mano, A. Aguiar-Ricardo, Green synthesis of a temperature sensitive hydrogel, Green Chem. 9 (1) (2007) 75–79, https://doi.org/10.1039/B603930H.
[24] M. Chellapandian, M.R.V. Krishnan, Chitosan-poly(glycidyl methacrilate) copolymer for immobilization of urease, Process Biochem. 33 (6) (1998) 595–600, https://doi.org/10.1016/S0032-9592(98)80001-0.

[25] A. Hirai, H. Odani, A. Nakajima, Determination of degree of deacetylation of chitosan by ^{1}H NMR spectroscopy, Polym. Bull. 26 (1991) 87–94, https://doi.org/10.1007/BF00299352.
[26] B. Yang, X. Li, S. Shi, X. Kong, G. Guo, M. Huang, F. Luo, Y. Wei, X. Zhao, Z. Qian, Preparation and characterization of a novel chitosan scaffold, Carbohydr. Polym. 80 (3) (2010) 860–865, https://doi.org/10.1016/j.carbpol.2009.12.044.
[27] I. Adekogbe, A. Ghanem, Fabrication and characterization of DTBP-crosslinked chitosan scaffolds for skin tissue engineering, Biomaterials 26 (35) (2005) 7241–7250, https://doi.org/10.1016/j.biomaterials.2005.05.043.
[28] D.R. Rohindra, A.V. Nand, J.R. Khurma, Swelling properties of chitosan hydrogels, S. Pac. J. Nat. Sci. 22 (1) (2004) 32–35, https://doi.org/10.1071/SP04005.
[29] UK RECOVERY trial. This is a Phase II/III randomised, controlled trial that began in March 2020, Which Is Testing Numerous Potential Treatments for Covid-19, Including Low-Dose Dexamethasone (6 Mg/Day). Dexamethasone Was Found to Reduce Deaths in Patients on Ventilators by One-Third and by One-Fifth in Patients Who Required Oxygen Only, https://www.recoverytrial.net (accessed 28.10.2020).
[30] S.E. Tsuei, R.G. Moore, J.J. Ashley, W.G. McBride, Disposition of synthetic glucocorticoids, I. Pharmacokinetics of dexamethasone in healthy adults, J. Pharmacokinet. Biopharm 7 (1979) 249–264, https://doi.org/10.1007/BF01060016.
[31] Y. Ikeda, B.S. Carson, D.M. Long, The effects of topical dexamethasone on experimental brain tumors and peritumoral brain oedema, Acta Neurochir. Suppl. (Wien) 51 (1990) 163–164, https://doi.org/10.1007/978-3-7091-9115-6_55.
[32] B. Mukherjee, S. Mahapatra, R. Gupta, B. Patra, A. Tiwari, P. Arora, A comparison between povidone-ethylcellulose and povidone-eudragit transdermal dexamethasone matrix patches based on in vitro skin permeation, Eur. J. Pharm. Biopharm. 59 (3) (2005) 475–483, https://doi.org/10.1016/j.ejpb.2004.09.009.
[33] C. Passot, M.F. Pouw, D. Mulleman, T. Bejan-Angoulvant, G. Paintaud, E. Dreesen, D. Ternant, Therapeutic drug monitoring of biopharmaceuticals may benefit from pharmacokinetic and pharmacokinetic-pharmacodynamic modeling, Ther. Drug Monit. 39 (4) (2017) 322–326, https://doi.org/10.1097/ftd.0000000000000389.